The Journal of Chemical Physics

RESEARCH ARTICLE | AUGUST 09 2019

Electron scattering from tin tetrachloride ($SnCl_4$) molecules

Paweł Możejko ; Sylwia Stefanowska-Tur; Elżbieta Ptasińska-Denga ; Czesław Szmytkowski

J. Chem. Phys. 151, 064305 (2019)
https://doi.org/10.1063/1.5116307

The Journal of Chemical Physics ARTICLE scitation.org/journal/jcp

Electron scattering from tin tetrachloride ($SnCl_4$) molecules

Cite as: J. Chem. Phys. 151, 064305 (2019); doi: 10.1063/1.5116307
Submitted: 24 June 2019 • Accepted: 19 July 2019 •
Published Online: 9 August 2019

Paweł Możejko,[a] Sylwia Stefanowska-Tur,[b] Elżbieta Ptasińska-Denga,[c] and Czesław Szmytkowski[d]

AFFILIATIONS

Department of Atomic, Molecular and Optical Physics, Faculty of Applied Physics and Mathematics, Gdańsk University of Technology, ul. Gabriela Narutowicza 11/12, 80-233 Gdańsk, Poland

[a]paw@pg.edu.pl
[b]sylstefa1@student.pg.edu.pl
[c]elzdenga@pg.edu.pl
[d]czsz@mif.pg.gda.pl

ABSTRACT

Absolute *grand*-total cross section (TCS) for electron scattering from a tin tetrachloride, $SnCl_4$, molecule was measured at electron-impact energies ranging from 0.6 to 300 eV, in the linear electron-transmission experiment. The measured TCS energy dependence shows two very pronounced enhancements peaking near 1.2 eV and around 9.5 eV, separated with a deep minimum centered close to 3 eV. The low energy structure is attributed to the formation of two short-living negative ion states. Additional weak structures in the TCS curve are also perceptible. We also calculated the integral elastic and ionization cross sections for $SnCl_4$ up to 4 keV within the additivity rule approximation and the binary-encounter-Bethe approach, respectively. To examine the role of the central atom of tetrachloride target molecules in collisions with electrons, we compared the experimental TCS energy functions for XCl_4 molecules (X = C, Si, Ge, Sn).

I. INTRODUCTION

Accurate experimental data concerning electron interactions, including scattering cross sections, with molecules in gas, liquid, and condensed phases, are very important for understanding variety of natural and technological processes occurring and carried on in complex environments. Such data are strongly desirable in studies of ionizing radiation to the biomolecules,[1–4] astrobiology,[5] and astrochemistry.[6–8] They are also of great importance for modern technologies including focused electron beam induced deposition (FEBID).[9,10]

Tin tetrachloride ($SnCl_4$) is one of the simplest molecular compounds which can be used as a precursor in nanostructure composition during FEBID. Despite the importance and potential applications of $SnCl_4$ in electron-beam based technologies, the knowledge of electron interactions with that compound is rather scarce and fragmentary. Experiments concerned mainly the investigation of electron-induced formation of positive[11] and negative ions.[12,13] For positive ions, relative abundances and appearance potentials were determined.[11] Low-energy spectra of anion fragments provided information on the resonant channel in the electron-$SnCl_4$ scattering.[12,13] Weak resonantlike features were observed[13] in the electron current transmitted through the $SnCl_4$ vapor, both measured and calculated. Unfortunately, intensities of investigated phenomena were presented in arbitrary units only, what makes difficulties in their applications for modeling the physico-chemical electron-assisted processes. From the theoretical point of view, most of electron-scattering data for $SnCl_4$ are available for intermediate and high energies; for very low energies, theoretical results remain sparse. Within 5–40 eV energy range, differential, integral, and momentum transfer cross sections for electron scattering from $SnCl_4$ were calculated employing the Schwinger multichannel method with pseudopotentials at the fixed-nuclei static-exchange approximation.[14] In the same work,[14] the ionization cross section calculated with the binary-encounter-Bethe method was reported from the threshold up to 500 eV. Inelastic and ionization cross sections were computed up to 5000 eV using the modified additivity rule (MAR) with the spherical complex optical potential (SCOP)

formalism and the complex scattering potential-ionization contribution (CSP-ic) approach, respectively.[15] Quite recently, the elastic and total cross sections calculated with the SCOP formalism were reported,[16] for energies from 20 to 5000 eV. Electron beams were also used to the molecular structure determination of tin tetrachloride in a few vapor-phase electron diffraction experiments (Ref. 17 and references therein).

The objective of the present work is to study electron interactions with the $SnCl_4$ molecule in collisions with energies ranging from low, where the possible resonant processes can dominate the scattering, to intermediate, at which all scattering channels are opened although two of them (elastic and ionization) dominate. Especially, we would like to provide reliable absolute electron-scattering total cross section (TCS) for the $SnCl_4$ molecule. For the explanation of the origin of the features visible in the measured TCS energy dependence, experimental data concerning particular e^-–$SnCl_4$ scattering events (available in the literature) as well as our calculations are employed. The measured TCS energy curve for $SnCl_4$ is then compared to TCS data for a series of tetrachloride XCl_4 (C, Si, Ge) molecules. Such comparison can reveal some regularities in the TCS behavior when going across this target family and give an insight into the role of a molecular structure in the scattering dynamics. Finally, we also calculated the integral elastic (ECS) and ionization cross sections (ICSs) up to 4 keV within the additivity rule (AR) approximation and the binary-encounter-Bethe (BEB) approach, respectively. Present calculations are confronted with other available computational results.

II. EXPERIMENTAL

Measurements of the absolute TCS for the electron scattering with tin tetrachloride molecules have been carried out using the electron spectrometer working in the linear transmission configuration under single collision conditions. The monoenergetic electron beam ($\Delta E \simeq 80$ meV) produced with an electron gun and a 127° cylindrical electrostatic condenser is directed with a system of electrostatic lenses into a scattering cell, which is filled with the studied target vapor. The electrons passing through the cell and getting across up to the exit orifice are energetically discriminated with the retarding-field analyzer unit, and finally, the transmitted electrons are collected with the Faraday cup detector. The Bouguer–Lambert attenuation formula (BL) allows us to determine the absolute total cross section, $Q(E)$, at each selected collision energy, E,

$$I_g(E) = I_0(E)\exp[-nLQ(E)],$$

where $I_g(E)$ and $I_0(E)$ are the intensities of the electron beam transmitted across the scattering cell taken with and without the target in the cell, respectively. L (=30.5 mm) is a path length of electrons in the reaction cell, while n is the number density of the target determined from the measurements of the gas target pressure and temperatures of the scattering cell and manometer head. As the temperature of the cell (310–320 K) differs slightly from the temperature of the capacitance manometer head (322 K), the correction due to the thermal transpiration effect[18,19] was taken into account. To ensure the absolute energy values, the experimental energy scale was calibrated against the well-known resonant oscillatory structure around 2.3 eV in molecular nitrogen;[20] overall inaccuracy of the electron energy scale is about 0.1 eV. The tin tetrachloride vapor has been obtained from a liquid sample (Aldrich) of 99.0% purity. Before the use, it was degassed in several freeze-pump-thaw cycles.

The electron spectrometer optics is maintained at a base pressure of 10^{-5} Pa. The magnetic field in the electron optics and interaction region is reduced by Helmholtz coils to the value below 0.1 μT. The temperature of the sample supplying line is kept at about 315 K to establish the thermal conditions near those in the reaction region. After opening/closing the gas valve, a relatively long delay was necessary to stabilize the target conditions in the scattering cell. This may generate some TCS uncertainty related to the target pressure determination. Further details of the measuring setup, experimental procedures, and data processing employed can be found in our earlier works.[21,22]

The final TCS value for each energy studied is an average of a large number of data measured in independent series (6–14) of individual runs (usually 10 in a series). Statistical uncertainties (one standard deviation of weighted mean values) are below 1% over the entire energy range used. The direct sum of all potential individual systematic errors, related to determination of quantities necessary to TCS derivation, has been estimated to be up to 10% at the lowest energies applied, decreasing gradually to about 5% between 10 and 100 eV and increasing to 6% at the highest collision energies we operated. The reported data are not corrected for the forward-scattering effect (cf. Ref. 23); however, the potential lowering of the TCS values related to that effect (estimated based on results of our calculations) is included in the overall systematic error.

III. COMPUTATIONAL METHODS

Theoretical methods and computational procedures applied in the present work are similar to those we used in previous calculations[24–26] including also studies on electron collisions with targets of tetrahedral symmetry.[27,28] Thus, only a brief description of the theoretical and numerical issues will be provided here.

To investigate the problem of elastic electron collisions with studied molecules, the additivity rule[29] based on the independent atom method (IAM)[30] was used. The integral elastic cross section (ECS) within the IAM method is given by

$$\sigma(E) = \sum_{i=1}^{N} \sigma_i^A(E), \tag{1}$$

where E is an energy of the incident electron and N is the number of atoms within the investigated molecule. The elastic cross section of the ith atom of the target molecule, $\sigma_i^A(E)$, was computed according to

$$\sigma^A = \frac{4\pi}{k^2}\left(\sum_{l=0}^{l_{max}}(2l+1)\sin^2\delta_l + \sum_{l=l_{max+1}}^{\infty}(2l+1)\sin^2\delta_l^{(B)}\right), \tag{2}$$

where $k = \sqrt{2E}$ is the wave number of the incident electron.

To obtain phase shifts, δ_l, partial wave analysis was employed and the radial Schrödinger equation

$$\left[\frac{d^2}{dr^2} - \frac{l(l+1)}{r^2} - 2(V_{stat}(r) + V_{polar}(r)) + k^2\right] u_l(r) = 0 \quad (3)$$

was solved numerically.

The electron-atom interaction was represented by the static, $V_{stat}(r)$,[31] and polarization, $V_{polar}(r)$,[32] potentials. In the present calculations, the exact phase shifts were calculated for up to $l_{max} = 50$, while those remaining, $\delta_l^{(B)}$, were included through the Born approximation.

The electron-impact ionization cross section was computed using the binary-encounter-Bethe (BEB) method.[33,34] Within this formalism, the electron-impact ionization cross section per molecular orbital is given by

$$\sigma^{BEB} = \frac{S}{t+u+1}\left[\frac{\ln t}{2}\left(1 - \frac{1}{t^2}\right) + 1 - \frac{1}{t} - \frac{\ln t}{t+1}\right], \quad (4)$$

where $u = U/B$, $t = T/B$, $S = 4\pi a_0^2 N R^2/B^2$, $a_0 = 0.5292$ Å, $R = 13.61$ eV, and T is the energy of the impinging electron.

The electron binding energy, B, kinetic energy of the orbital, U, and orbital occupation number, N, were obtained for the ground states of the molecules with the Hartree-Fock method using the GAUSSIAN code[35] and the augmented correlation-consistent polarized valence-triple-zeta (aug-cc-pVTZ) basis set.[36] For Sn atom, the small-core, relativistic energy-consistent pseudopotential[37] with corresponding aug-cc-pVTZ-pp basis set[38] were used.

Because energies of the highest occupied molecular orbitals (HOMOs) obtained in this way usually differ slightly from experimental ones, we performed also outer valence Green function calculations of correlated electron affinities and ionization potentials[39,40] with the GAUSSIAN code.[35] The experimental value[11] of the first ionization potential (11.5 eV) was inserted in the calculation, instead of that calculated (12.35 eV), to fix the threshold behavior of the ionization cross section at the experimental value. The calculated values of B, U, and N for selected molecular orbitals are presented in Table I. Since orbitals with high binding energies do not contribute much to total ionization cross section, they were omitted in Table I although we included them in calculations.

TABLE I. Electron binding energies B, kinetic energies of the orbitals U, and orbital occupation number N for molecular orbitals of the $SnCl_4$ molecule.

Orbital symmetry	B (eV)	U (eV)	N
a_1	162.7	69.63	2
t_2	113.5	102.1	6
t_2	39.31	139.8	6
e	39.07	142.5	4
a_1	30.88	72.16	2
t_2	29.90	87.77	6
a_1	17.58	49.29	2
t_2	14.36	53.55	6
e	12.89	58.52	4
t_2	12.56	62.51	6
t_1	12.35	62.04	6

The cross section for electron-impact ionization of the molecule (ICS) can be obtained as the sum of σ^{BEB} for all molecular orbitals n_{MO},

$$\sigma^{Ion} = \sum_{i=1}^{n_{MO}} \sigma_i^{BEB}. \quad (5)$$

The sum of the computed elastic (ECS) and ionization (ICS) cross sections can represent the theoretical total electron-scattering cross section for molecule; ECS+ICS is used for comparison with present experimental TCS data and other calculations.

IV. RESULTS AND DISCUSSION

In this section, we present our absolute *grand*-total electron-scattering cross sections (TCSs) for the $SnCl_4$ molecule measured in the electron-transmission experiment over the incident energy ranging from 0.6 to 300 eV. Observed TCS features are explained based on the electron-scattering data available for the considered compound. To examine how the central atom in the tetrachloride molecule influences the electron-molecule scattering, we compare TCS energy dependence for the $SnCl_4$ molecule with present experimental TCS data for the family of XCl_4 (X = C, Si, Ge) targets: CCl_4,[41] $SiCl_4$,[42] and $GeCl_4$.[43] Similarities and differences of the compared TCS energy functions are pointed out. Finally, we also present our calculated integral elastic (ECS) and ionization (ICS) cross sections for electron collision with the $SnCl_4$ molecules, for energies up to 4 keV. The sum, ECS+ICS, is then compared with the measured TCS.

A. Cross sections for tin tetrachloride [$SnCl_4$]

Figure 1 shows absolute total cross section (TCS) as a function of the incident electron energy measured for the $SnCl_4$ molecule in the range 0.6–300 eV; numerical TCS values are collected in

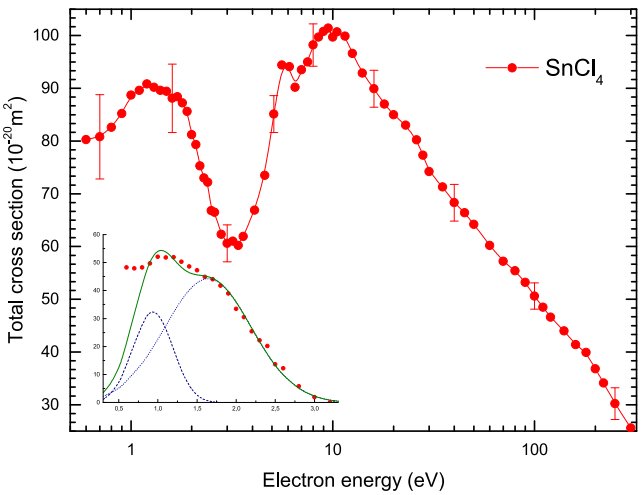

FIG. 1. Experimental total cross section, full (red) circles, for the electron scattering from the $SnCl_4$ molecule; line added to guide the eyes. Error bars correspond to overall experimental uncertainties. The inset shows decomposition of the first TCS enhancement into two Gaussian curves; please note that the estimated direct scattering contribution is subtracted here from the TCS.

Table II. No experimental absolute electron-scattering TCS data for the investigated molecule are available in the literature for comparison.

The characteristic feature of the measured TCS for the $SnCl_4$ molecule is its relatively high magnitude over the whole energy range investigated. The TCS value varies between 101×10^{-20} m^2 in its maximum around 10 eV and almost 26×10^{-20} m^2 at 300 eV. Such high TCS reflects in part the large geometrical size of the target molecule; the gas kinetic cross section, σ_{gk}, for $SnCl_4$ amounts of 20.2×10^{-20} m^2 (see Table IV).

With respect to the general shape, the TCS energy function is dominated by two prominent enhancements separated with a narrow deep minimum centered near 3 eV. The first, narrow ($\Delta E \simeq 1$ eV, FWHM) TCS enhancement has a maximum of the value about 90×10^{-20} m^2 located around 1.2 eV. On the right from this maximum, near 1.7 eV, a weak shoulder is visible leading to distinct flattening of the peak. Such appearance of the low-energy TCS enhancement suggests that it can be composed of two narrow structures. In fact, this enhancement can be reproduced with two Gaussian curves (see inset in Fig. 1) peaking at 0.94 and 1.64 eV (the width of 0.5 and 1.1 eV, FWHM), respectively. The presence of two features in this energy regime (localized at 0.9 and 1.6 eV) was also noticed by Modelli *et al.*[13] in the derivative of the electron current transmitted through $SnCl_4$ as a function of the incident energy (ET spectrum). On the other hand, the derivative of the calculated total cross section[13] shows only a single feature, located within 0.9 and 1.6 eV.

The second TCS enhancement is very broad and highly asymmetric. Starting from the minimum value of about 60×10^{-20} m^2 near 3.1 eV, the TCS energy function rises sharply, peaking in the vicinity of 5.6 eV with an intensity of about 94×10^{-20} m^2. The amplitude of this narrow structure, against a smoothly increasing TCS *background*, is quite remarkable and amounts to about 10×10^{-20} m^2. On the right from the TCS peak at 5.6 eV, a weak minimum appears near 6.5 eV. With a further increase in the electron impact energy, the TCS energy function increases again and reaches its maximum value of nearly 101×10^{-20} m^2 close to 9.5 eV. Above 10 eV, the TCS decreases rather smoothly to about 26×10^{-20} m^2 at the highest energy used, 300 eV; only around 25 eV, some change in the slope of the curve is discernible.

Considering the shape of the low-energy TCS dependence, we can state that below 10 eV resonant processes are involved in the electron–$SnCl_4$ scattering. The resonant electron scattering proceeds via creation of the temporary compound of the impinging electron of appropriate energy and the target molecule. The resulting parent negative-ion state (resonance) can decompose either through the simple autodetachment of the extra electron[44] and/or via dissociation to negative and neutral fragments.[45] The electron detachment leads to structures visible in the elastic and vibrational cross sections, while the dissociative (DA) channel manifests in the negative ion spectra.

Evidences on the resonant electron–$SnCl_4$ scattering character at low impact energies are rather scarce. Below 2 eV, the only support for the appearance of a low-energy resonant phenomenon comes from experiments and calculations of Modelli *et al.*[13] In the electron transmission spectrum (ET), Modelli and co-workers observed two features located at 0.9 and 1.6 eV. Based on MS-Xα calculations, they related these features to formation of resonances associated with two empty $SnCl_4$ orbitals, both of t_2 symmetry. In the DA spectrum, around 0.7 eV, Modelli *et al.* observed a weak $SnCl_3^-$ fragment signal and associated it with the t_2 resonance visible at 0.9 eV in the ET spectrum. Present computations carried out with the Partial Third Order (P3) propagator[35] reveal two low-energy unoccupied molecular orbitals of a_1 and t_2 symmetry located at 0.717 and 1.026 eV, respectively (cf. Fig. 2). We suggest that both orbitals can be involved in the resonances responsible for the structures observed around 1.2 eV in the experimental TCS (Fig. 1). The spatial character of these orbitals (see Fig. 2) suggests that the first resonance can decompose via electron autodetachment, while the second can be dissociative. It is interesting that no negative ion was detected within 0 and 2 eV electron impact energy by Pabst *et al.*[12] It should be noted that according to present P3 calculations, the lowest unoccupied molecular orbital of a_1 symmetry lies below zero energy, at −1.021 eV; this corresponds to the value of −0.8 eV obtained with the MS-Xα calculations.[13] Both theoretical results predict that the ground state of the $SnCl_4^-$ anion should be stable.

TABLE II. Absolute experimental electron-scattering total cross sections (TCSs), at impact energy E (in eV), for the tin tetrachloride ($SnCl_4$) molecule; in units of 10^{-20} m^2.

E	TCS	E	TCS	E	TCS	E	TCS
0.6	80.2	2.3	73.0	8.1	98.2	40	68.3
0.7	80.8	2.4	72.2	8.6	99.7	45	66.4
0.8	82.6	2.5	66.8	9.1	100.8	50	64.2
0.9	85.2	2.6	66.5	9.6	101.4	60	60.2
1.0	88.7	2.8	62.3	10	99.7	70	57.2
1.1	89.6	3.0	60.6	10.5	100.7	80	55.4
1.2	90.8	3.2	60.9	11.5	99.9	90	53.2
1.3	90.2	3.4	60.2	12.5	96.6	100	50.7
1.4	89.6	3.6	61.9	15	92.9	110	48.5
1.5	89.4	4.1	66.9	17	89.9	120	46.6
1.6	88.1	4.6	73.5	19	87.0	140	44.0
1.7	88.4	5.1	85.1	21	85.0	160	41.4
1.8	87.2	5.6	94.4	23	83.0	180	39.9
1.9	85.6	6.1	94.1	26	80.2	200	36.8
2.0	81.2	6.6	90.9	28	77.3	220	34.1
2.1	79.3	7.1	93.5	30	74.2	250	30.2
2.2	75.3	7.6	95.0	35	71.3	300	25.7

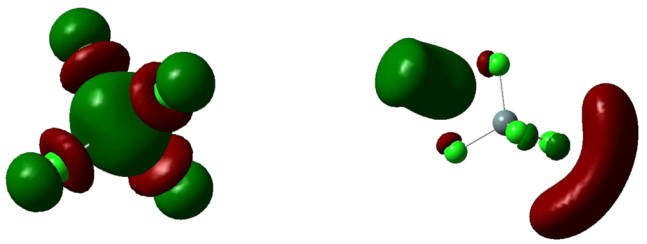

FIG. 2. The second and the third lowest unoccupied molecular orbital of the $SnCl_4$ molecule.

Beyond 3 eV, the resonant contribution to the electron-$SnCl_4$ scattering is better documented. In the vicinity of 4.5 eV, fragment anions ($SnCl_3^-$ and Cl^-) were observed in experiments of Pabst *et al.*[12] and Modelli *et al.*[13] In addition, Pabst and co-workers detected also $SnCl_2^-$ and Cl_2^- fragments around 4 eV and 5.5 eV, respectively. A narrow resonant feature centered at 5.24 eV was visible in the TE spectrum of $SnCl_4$ taken by Modelli *et al.*[13] In this energy regime, they also detected the occurrence of the parent molecular anion, $SnCl_4^-$. All aforementioned resonant features are located in the range of the distinct structure visible in the present TCS energy curve, peaking in the vicinity of 5.6 eV (see Fig. 1). Modelli *et al.* suggested that within 4–6 eV the temporary molecular anion state is formed when the electron capture is accompanied by electronic excitation of the target molecule through a core-excited resonance.[13]

To complement the presented low-energy e^-–$SnCl_4$ scattering data, it is worth mentioning that the integral elastic cross section (IECS) calculated by Joucoski and Bettega[14] (see in Fig. 3) shows a maximum (~66 × 10^{-20} m^2) near 7 eV followed with a broad enhancement peaking near 16 eV with the value of about 70 × 10^{-20} m^2.

Figure 3 confronts present measured TCS with calculated total and partial (elastic, ionization, and inelastic) cross sections available in the literature for the electron scattering from the $SnCl_4$ molecule. Present computed elastic (ECS) and ionization (ICS) cross sections (see Table III) along with their sum ECS+ICS are also depicted for the comparison.

From Fig. 3, it is clear that in the range of 30–300 eV, where energies of measurements and computations overlap, both curves representing theoretical total cross section (the present one and that of Ref. 16) lie systematically below the experimental TCS values. However, present calculated total cross sections are closer to the experimental findings than those calculated in Ref. 16. The differences between present measured TCS and calculated values reach about 20% around 50 eV and 15% near 200 eV. The lowering of present calculated ECS+ICS values with respect to the experimental TCS is associated with the neglection in our calculations of the multiple and dissociative ionization as well as the excitation of

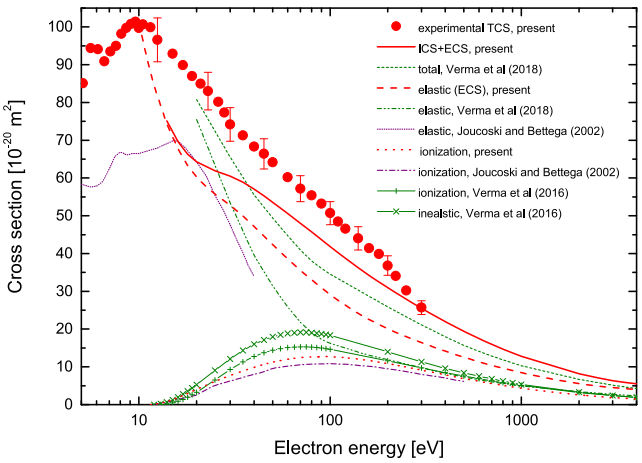

FIG. 3. Comparison of the absolute total cross sections (TCSs) for electron–$SnCl_4$ scattering obtained in the present experiment, full (red) circles, with calculated cross sections. Elastic (ECS): long dash (red) line, present; dashed-double dotted (olive) line;[16] short dotted (purple) line.[14] Ionization (ICS) computed: dotted (red) line, present; dashed-double dotted (purple) line;[14] full (olive) line with +.[15] Inelastic, computed: full (olive) line with ×.[15] Total, computed: heavy (red) line, ECS+ICS, present; short dashed (olive) line.[16]

TABLE III. Calculated ionization (ICS) and elastic (ECS) cross sections for electron scattering from the $SnCl_4$ molecule in units of 10^{-20} m^2.

E	ICS	ECS	*E*	ICS	ECS	*E*	ICS	ECS
11.5	0.0		55	11.70		275	9.522	
12.0	0.0898		60	12.03	38.56	300	9.136	16.41
13.0	0.354		65	12.28		350	8.448	15.16
14.0	0.799	74.33	70	12.46	35.54	400	7.856	14.14
15.0	1.325		75	12.59		450	7.343	13.28
16.0	1.891	67.73	80	12.66	33.06	500	6.896	12.55
17.0	2.443		85	12.71		600	6.154	11.34
18.0	2.985	63.30	90	12.72	30.96	700	5.564	10.40
19.0	3.517		95	12.71		800	5.084	9.633
20.0	4.023	60.26	100	12.68	29.17	900	4.684	8.996
22.5	5.169		110	12.58	27.63	1000	4.347	8.456
25.0	6.154	55.8	120	12.44	26.30	1500	3.221	
27.5	6.996		140	12.08	24.16	2000	2.579	5.597
30.0	7.717	52.77	160	11.68	22.51	2500	2.161	4.932
35.0	8.960	49.93	180	11.27	21.19	3000	1.865	4.495
40.0	9.910	47.16	200	10.87	20.09	3500	1.645	4.215
45.0	10.67	44.61	225	10.39		4000	1.473	4.058
50.0	11.26	42.34	250	9.939	17.98			

molecules induced in the scattering. Calculations of Verma *et al.*[15] show (cf. Fig. 3) that in the energy range 50–300 eV, their total ionization cross sections distinctly exceed (by 10%–25%) ICS values obtained in the present calculations and those of Joucoski and Bettega[14] with the BEB model, in which multiple and dissociative ionization processes are neglected. In the same work,[15] Verma *et al.* demonstrated also a significant role of the excitation processes in the electron–$SnCl_4$ scattering; their calculated cross sections for the inelastic scattering are higher than those for the total ionization by 12%–25%.

B. Comparison of TCSs for XCl_4 molecules (X = C, Si, Ge, Sn)

In this section, we compare experimental TCSs energy curves for a series of tetrachloride molecules with the central atom from the carbonic (14) group: C, Si, Ge, and Sn (see Fig. 4).

Figure 4 shows that the general energy dependence of all compared TCS functions is very similar. Each TCS curve depicted in Fig. 4 has two pronounced enhancements separated with a deep minimum centered within 2.9–3.3 eV. The first, narrow low-energy TCS peak is centered at 1.2 eV for CCl_4, near 1.9 eV for $SiCl_4$ and $GeCl_4$ and close to 1.2 eV for the $SnCl_4$ molecule (cf. Table IV). For each compared molecule, these peaks were associated[13] with short-lived resonant states created when the incident electron is captured into an unoccupied molecular orbital of the t_2 symmetry. Recently, the dissociative character of these resonant states was confirmed; the formation of CCl_3^- and CCl_2^- fragment anions from CCl_4 (between 1.2 eV and 1.8 eV), $SiCl_2^-$ and Cl^- from $SiCl_4$ (between 1.8 eV and 2.1 eV) and $GeCl_3^-$ and Cl_2^- from $GeCl_4$ (around 1.4 eV) was observed in a crossed electron-molecule beam experiment.[46] The second, very broad enhancement peaks at 7.5 eV for CCl_4, within 9.5–10 eV for $SiCl_4$ and $GeCl_4$ and at 9.5 eV for $SnCl_4$ (see Table IV). Some differences between compared TCS curves appear on both slopes of the broad enhancement. On the right-hand side from the TCS maximum for CCl_4, near 10 eV, a distinct shoulder is visible. In contrary, for $SiCl_4$, a small peak appears on the low-energy slope of the enhancement, near 5.5 eV. The TCS for $GeCl_4$ shows a weak shoulder near 7.5 eV, and the $SnCl_4$ curve has a peak close to 5.6 eV.

More distinct differences are visible in the magnitude of compared TCSs. From Fig. 4, it is clear that the magnitude of TCS for

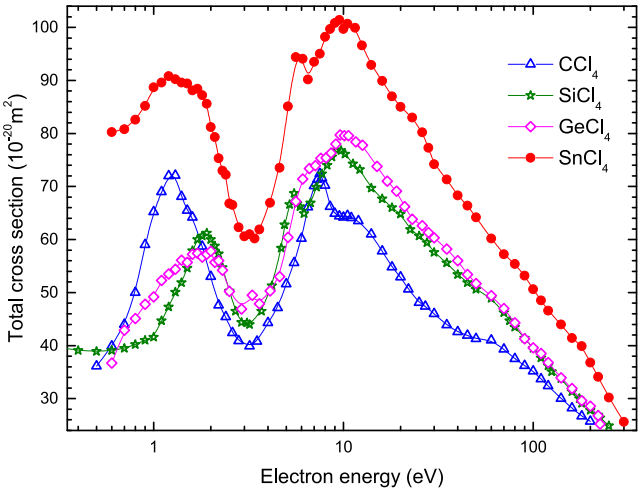

FIG. 4. Comparison of experimental total cross sections for the electron scattering from the XCl_4 molecules (X = C, Si, Ge, Sn): full (red) circles, $SnCl_4$, present; open (magenta) diamonds, $GeCl_4$, from Ref. 43; open (olive) stars, $SiCl_4$, from Ref. 42; open (blue) triangles, CCl_4, from Ref. 41; lines are added to guide the eyes.

$SnCl_4$ distinctly exceeds other depicted TCSs over the whole investigated energy range. Below 10 eV, where resonant processes predominate the scattering, for all molecules examined, except $SnCl_4$, there is no clear relationship between physico-chemical molecular parameters and the TCS magnitude. For example, around 1.5 eV, the TCS magnitude for the smallest molecule, CCl_4, lies distinctly above those for $SiCl_4$ and $GeCl_4$. On the other hand, TCS curves for the two last-mentioned molecules do not differ too much in the shape and magnitude. Such similarity in TCSs was also noticed for permethylated compounds $Si(CH_3)_4$ and $Ge(CH_3)_4$.[28]

Figure 5 shows that above 10 eV, where the role of resonant processes in the electron scattering is not significant, the higher TCS corresponds to the larger molecular size (see Table IV). It is interesting that in the vicinity of 3 eV, where each TCS has its local minimum, the order of the TCS magnitudes is also related to the size of molecule. This indicates that in this energy regime, resonant contributions are less important. Very similar trend of TCS

TABLE IV. Location of the low-energy features, E_{TCS} and E_{ETS}, perceptible in the TCS energy dependences taken in our laboratory for considered molecules and in the ET spectra of Modelli *et al.*,[13] respectively. Gas kinetic cross sections, σ_{gk}, are calculated from van der Waals' constant, *b*;[48] the static polarizabilities of molecules, α, are from Ref. 49.

Molecule	E_{TCS} (eV)	E_{ETS} (eV)	σ_{gk} 10^{-20} m^2	α 10^{-30} m^3
$SnCl_4$	(1.1 − 1.3; 1.7; 5.6)[a]	(0.9; 1.6; 5.2)	20.2	18.1
$GeCl_4$	(1.7 − 2; 10)[b]	(1.7; 5.6)	18.9	15.1
$SiCl_4$	(1.9; 5.5; 9.5)[c]	(1.15; 2.1; 5.4)	18.7	12.9
CCl_4	(1.2; 7.5)[d]	(0.94)	17.1	11.2

[a]Present work.
[b]Reference 43.
[c]Reference 42.
[d]Reference 41.

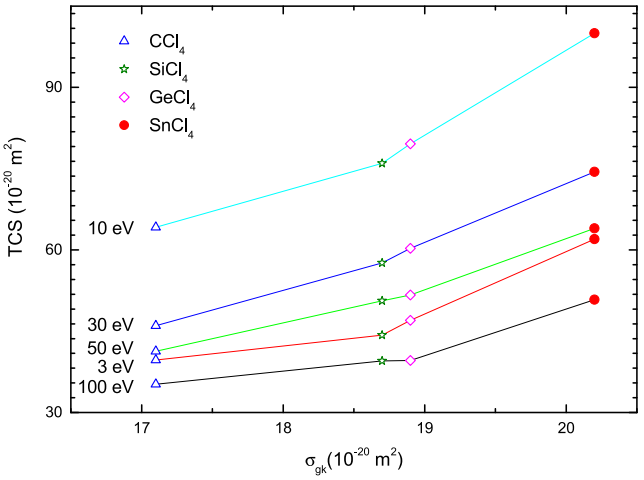

FIG. 5. Experimental total cross sections (TCSs) for the electron scattering from the XCl_4 molecules (X = C, Si, Ge, Sn) vs gas kinetic cross sections, σ_{gk} (cf. Table IV): full (red) circles, $SnCl_4$, present; open (magenta) diamonds, $GeCl_4$, from Ref. 43; open (olive) stars, $SiCl_4$, from Ref. 42; open (blue) triangles, CCl_4, from Ref. 41.

magnitude for considered compounds with their electric polarizability is also observed. The latter is consistent with recent findings on the correlation of TCS magnitude with molecular polarizability for the linear primary alcohols.[47]

It is worth noting that our observation on general increase in the TCS magnitude with the size of the tetrachloride molecule is in some conflict with the conclusion of Joucoski and Bettega based on their calculations.[14] They found that a change in the central atom for tetrachlorides increases the integral elastic cross section (IECS) by a small amount. In fact, their IECSs between 25 and 30 eV nearly coincide, however, at 40 eV the IECS for $SnCl_4$ is about 15% lower then those for $SiCl_4$ and $GeCl_4$.

V. CONCLUSIONS

We have presented our experimental absolute total cross sections for electron scattering from $SnCl_4$ molecules measured over an energy range from 0.6 to 300 eV. The most characteristic features of the measured TCS are (i) relatively high magnitude over whole energy range used. At the maximum, around 9.5 eV, the value of TCS slightly exceeds 100×10^{-20} m^2; (ii) two very pronounced enhancements. They peak near 1.2 eV and around 9.5 eV and are separated with the deep minimum located close to 3 eV. Additional weak structures in the TCS curve are also visible. Analysis reveals that the first low energy structure can be attributed to the formation of two resonant states located at around 0.94 eV and 1.64 eV. Based on available electron scattering data for the $SnCl_4$ molecule and present calculations, we attributed the TCS low-energy features to the formation of short-living negative ion states. However, for better understanding the role of different processes that may occur in the electron–$SnCl_4$ scattering, further studies are highly desirable, especially those concerning the vibrational excitation.

To examine the role of the central atom of tetrachloride target molecules in the electron scattering, we compared the measured TCS energy functions for XCl_4 molecules (X = C, Si, Ge, Sn). While going across the XCl_4 series, at impact energies where resonant processes are negligible, the TCS increases with the molecular size of the target molecule.

In addition, for the $SnCl_4$ molecule, the integral elastic (ECS) and ionization (ICS) cross sections have been calculated at intermediate and high electron-impact energies in the additivity rule approximation and the binary-encounter-Bethe approach, respectively. The sum ECS+ICS appears to be systematically lower than the measured TCS.

ACKNOWLEDGMENTS

This work has been supported in part by the Polish Ministry of Science and Higher Education (MNiSzW Project 2018–2019). This research is part of the COST Action No. CM1301 (CELINA). Sylwia Stefanowska-Tur kindly acknowledges the support of the Polish Ministry of Science and Higher Education within the Diamond Grant program (Project No. DI2015 018945). Numerical calculations have been performed at the Academic Computer Center (TASK) in Gdańsk.

REFERENCES

[1] L. Sanche, Nature **461**, 358 (2009).
[2] J. D. Gornfinkiel and S. Ptasińska, J. Phys. B: At., Mol. Opt. Phys. **50**, 182001 (2017).
[3] A. I. Lozano, J. C. Oller, D. B. Jones, R. F. da Costa, M. T. do N. Varella, M. H. F. Bettega, F. Ferreira da Silva, P. Limão-Vieira, M. A. P. Lima, R. D. White, M. J. Brunger, F. Blanco, A. Muñoz, and G. Garcia, Phys. Chem. Chem. Phys. **20**, 22368 (2018).
[4] A. D. McKee, M. J. Schaible, R. A. Rosenberg, S. Kundu, and T. M. Orlando, J. Chem. Phys. **150**, 204709 (2019).
[5] K. Altwegg, H. Balsiger, A. Bar-Nun, J.-J. Bertheller, A. Bieler, P. Bochsler, C. Briois, U. Calmonte, M. R. Combi, H. Cottin, J. De Keyser, F. Dhooghe, B. Fiethe, S. A. Fuselier, S. Gase, T. I. Gombosi, K. C. Hansen, M. Haessig, A. Jäckel, E. Kopp, A. Korth, L. Le Roy, U. Mall, B. Marty, O. Mousis, T. Owen, H. Réme, M. Rubin, T. Sémon, C.-Y. Tzou, J. H. Waiter, and P. Wurz, Sci. Adv. **2**, e1600285 (2016).
[6] L. Campbell and M. J. Brunger, Int. Rev. Phys. Chem. **35**, 297 (2016).
[7] S. Esmaili, A. D. Bass, P. Cloutier, L. Sanche, and M. A. Huels, J. Chem. Phys. **148**, 164702 (2018).
[8] K. E. Shulenberger, J. L. Zhu, K. Tran, S. Abdullahi, C. Belvin, J. Lukens, Z. Peeler, E. Mullikin, H. M. Cumberbatch, J. Huang, K. Regovich, A. Zhou, L. Heller, M. Markovic, L. Gates, C. Buffo, R. Tano-Menka, C. R. Arumainayagam, E. Böhle, P. Swiderek, S. Esmaili, A. D. Bass, M. Huels, and L. Sanche, ACS Earth Space Chem. **3**, 800 (2019).
[9] S. Engmann, M. Stano, P. Papp, M. J. Brunger, Š. Matejčik, and O. Ingólfsson, J. Chem. Phys. **138**, 044305 (2013).
[10] M. Huth, F. Porrati, and O. V. Dobrovolskiy, Microelectron. Eng. **185-186**, 9 (2018).
[11] A. S. Buchanan and D. J. Knowels, J. Phys. Chem. **78**, 4394 (1969).
[12] R. E. Pabst, D. L. Perry, J. L. Margrave, and J. L. Franklin, Int. J. Mass Spectrom. Ion Phys. **24**, 323 (1977).
[13] A. Modelli, M. Guerra, D. Jones, G. Distefano, and M. Tronc, J. Chem. Phys. **108**, 9004 (1998).
[14] E. Joucoski and M. H. F. Bettega, J. Phys. B: At., Mol. Opt. Phys. **35**, 4953 (2002).
[15] P. Verma, D. Mahato, J. Kaur, and B. Antony, Phys. Plasmas **23**, 093512 (2016).
[16] P. Verma and B. Antony, J. Electron Spectrosc. Relat. Phenom. **222**, 51 (2018).

[17]H. Fujii and M. Kimura, Bull. Chem. Soc. Jpn. **43**, 1933 (1970).
[18]M. Knudsen, Ann. Phys. **336**, 205 (1910).
[19]K. F. Poulter, M. J. Rodgers, P. J. Nash, T. J. Thompson, and M. P. Perkin, Vacuum **33**, 311 (1983).
[20]Cz. Szmytkowski, K. Maciąg, and G. Karwasz, Phys. Scr. **54**, 271 (1996).
[21]Cz. Szmytkowski, P. Możejko, and G. Kasperski, J. Phys. B: At., Mol. Opt. Phys. **31**, 3917 (1998).
[22]Cz. Szmytkowski and P. Możejko, Vacuum **63**, 549 (2001).
[23]M. J. Brunger, S. J. Buckman, and K. Ratnavelu, J. Phys. Chem. Ref. Data **46**, 023102 (2017).
[24]P. Możejko and L. Sanche, Radiat. Environ. Biophys. **42**, 201 (2003).
[25]Cz. Szmytkowski, A. Domaracka, P. Możejko, E. Ptasińska-Denga, Ł. Kłosowski, M. Piotrowicz, and G. Kasperski, Phys. Rev. A **70**, 032707 (2004).
[26]Cz. Szmytkowski, A. Domaracka, P. Możejko, E. Ptasińska-Denga, and S. Kwitnewski, J. Phys. B: At., Mol. Opt. Phys. **38**, 745 (2005).
[27]P. Możejko, B. Żywicka-Możejko, and Cz. Szmytkowski, Nucl. Instrum. Methods Phys. Res., Sect. B **196**, 245 (2002).
[28]S. Stefanowska-Tur, P. Możejko, E. Ptasińska-Denga, and Cz. Szmytkowski, J. Chem. Phys. **150**, 094303 (2019).
[29]D. Raj, Phys. Lett. A **160**, 571 (1991).
[30]N. F. Mott and H. S. W. Massey, *The Theory of Atomic Collisions* (Oxford University Press, Oxford, 1965).
[31]F. Salvat, J. D. Martinez, R. Mayol, and J. Parellada, Phys. Rev. A **36**, 467 (1987).
[32]N. T. Padial and D. W. Norcross, Phys. Rev. A **29**, 1742 (1984).
[33]W. Hwang, Y. K. Kim, and M. E. Rudd, J. Chem. Phys. **104**, 2956 (1996).
[34]H. Tanaka, M. J. Brunger, L. Campbell, H. Kato, M. Hoshino, and A. R. P. Rau, Rev. Mod. Phys. **88**, 025004 (2016).
[35]M. J. Frisch, G. W. Trucks, H. B. Schlegel, G. E. Scuseria, M. A. Robb, J. R. Cheeseman, G. Scalmani, V. Barone, B. Mennucci, G. A. Petersson, H. Nakatsuji, M. Caricato, X. Li, H. P. Hratchian, A. F. Izmaylov, J. Bloino, G. Zheng, J. L. Sonnenberg, M. Hada, M. Ehara, K. Toyota, R. Fukuda, J. Hasegawa, M. Ishida, T. Nakajima, Y. Honda, O. Kitao, H. Nakai, T. Vreven, J. A. Montgomery, Jr., J. E. Peralta, F. Ogliaro, M. Bearpark, J. J. Heyd, E. Brothers, K. N. Kudin, V. N. Staroverov, T. Keith, R. Kobayashi, J. Normand, K. Raghavachari, A. Rendell, J. C. Burant, S. S. Iyengar, J. Tomasi, M. Cossi, N. Rega, J. M. Millam, M. Klene, J. E. Knox, J. B. Cross, V. Bakken, C. Adamo, J. Jaramillo, R. Gomperts, R. E. Stratmann, O. Yazyev, A. J. Austin, R. Cammi, C. Pomelli, J. W. Ochterski, R. L. Martin, K. Morokuma, V. G. Zakrzewski, G. A. Voth, P. Salvador, J. J. Dannenberg, S. Dapprich, A. D. Daniels, O. Farkas, J. B. Foresman, J. V. Ortiz, J. Cioslowski, and D. J. Fox, GAUSSIAN 09, Revision D.01, Gaussian, Inc., Wallingford, CT, 2009.
[36]D. E. Woon and T. H. Dunning, Jr., J. Chem. Phys. **98**, 1358 (1993).
[37]B. Metz, H. Stoll, and M. Dolg, J. Chem. Phys. **113**, 2563 (2000).
[38]K. A. Peterson, J. Chem. Phys. **119**, 11099 (2003).
[39]L. S. Cederbaum, J. Phys. B **8**, 290 (1975).
[40]V. G. Zakrzewski and W. von Niessen, J. Comput. Chem. **14**, 13 (1994).
[41]Cz. Szmytkowski, A. M. Krzysztofowicz, P. Janicki, and L. Rosenthal, Chem. Phys. Lett. **199**, 191 (1992).
[42]P. Możejko, G. Kasperski, Cz. Szmytkowski, A. Zecca, G. P. Karwasz, L. Del Longo, and R. S. Brusa, Eur. Phys. J. D **6**, 481 (1999).
[43]Cz. Szmytkowski, P. Możejko, and G. Kasperski, J. Phys. B: At., Mol. Opt. Phys. **30**, 4363 (1997).
[44]A. Herzenberg, in *Electron-Molecule Collisions*, edited by I. Shimamura and K. Takayanagi (Plenum Press, London, NY, 1984).
[45]R. N. Compton and J. N. Bardsley, in *Electron-Molecule Collisions*, edited by I. Shimamura and K. Takayanagi (Plenum Press, London, NY, 1984).
[46]T. P. Ragesh Kumar, B. Brynjarsson, B. Ómarsson, M. Hoshino, H. Tanaka, P. Limão-Vieira, D. B. Jones, M. J. Brunger, and O. Ingólfsson, Int. J. Mass Spectrom. **426**, 12 (2018).
[47]M. Gomes, D. G. M. da Silva, A. C. P. Fernandes, S. Ghosh, W. A. D. Pires, D. B. Jones, F. Blanco, G. Garcia, M. J. Brunger, and M. C. A. Lopes, J. Chem. Phys. **150**, 194307 (2019).
[48]*Handbook of Chemistry and Physics*, 76th ed., edited by D. R. Lide (CRC Press, Boca Raton, 1995-1996).
[49]M. Gussoni, M. Rui, and G. Zerbi, J. Mol. Struct. **447**, 163 (1998).